

A Physicochemical Study of Coke Formation on [Al]-ZSM-5 and Its Gallium(III) and Iron(III) Isomorphs during Methanol Conversion

G. PAUL HANDRECK AND THOMAS D. SMITH¹

Chemistry Department, Monash University, Clayton, Victoria, Australia 3168

Received June 20, 1989; revised January 16, 1990

The progress of coke formation on samples of the zeolite H-[Al]-ZSM-5, Si/Al ratios of 27 and 39, during their use in the conversion of methanol to hydrocarbons has been monitored by measurement of (a) the coke content of the zeolite as a function of the quantity of methanol feed, (b) zeolitic ion-exchange capacities at various coke loadings, and (c) the adsorption of methylene blue on the surface of the zeolite containing various amounts of coke. Similar measurements have been made on the coking of the gallium(III) and iron(III) isomorphs of ZSM-5 which occurs during methanol conversion and on the coking of H-[Al]-ZSM-5 during its use in mesitylene cracking. The results of such measurements show that the acid site coverage per unit quantity of coke in the early stages of coking follows the order of increasing Brønsted acidity, namely Fe(III) < Ga(III) < Al(III); coke formation involves some aggregation of coke material on the surface of the zeolite; the coking of H-[Al]-ZSM-5 is greatly influenced by its Al(III) content; and coking occurs only to a minor extent as a result of mesitylene cracking on H-[Al]-ZSM-5. © 1990 Academic Press, Inc.

INTRODUCTION

An important feature of zeolite ZSM-5 is the low rate of coking which takes place during hydrocarbon conversions compared to that observed using erionite (1), chabazite (1), zeolite Y (2, 3), offretite (4), mordenite (4, 5), and erionite/offretite (6), thus requiring less frequent regeneration (7). Oxidative regeneration of the coked zeolite ZSM-5 has been found to be slow when compared with that observed for zeolite Y and mordenite (8). Removal of coke deposits by contact with a stream of ozone (9, 10) or nitrous oxide (11, 12) has been put forward as successful treatment for the regeneration of zeolite ZSM-5.

By the use of high-resolution ¹³C NMR spectroscopy, a range of aliphatic and aromatic products formed in the conversion of methanol over zeolite ZSM-5 were found to be trapped within the channel structure while the acid sites were tenanted by alkoxide species (13). Analysis of the coke after dissolution of the zeolite material in hydrof-

luoric acid showed it to consist of alkylated mono- and binuclear aromatic molecules (2, 14) while the hydrogen-to-carbon ratio fell from about 2.5 to 1.0 as the time of exposure to methanol increased (14, 15).

It has been claimed that coke forms on the external surface of the zeolite, leading to modified shape selectivity and finally to catalyst deactivation by pore blocking (4). In addition, the view has been expressed that while coking occurs initially on the external surface after the conversion has proceeded for some time (100 h), coke is deposited within the channels as a result of alkene polymerization (1). Alternatively, evidence gathered from dinitrogen sorption (16), ammonia and pyridine chemisorption (17, 18), and X-ray photoelectron spectroscopy (19) indicated that coke was formed initially within the zeolite channels during the catalytic conversion of methanol and finally on the external surface after hydrocarbon production had ceased. This view has since been modified to include some external coke formation at low coke loadings (6%) as observed by transmission electron microscopy (20). More detailed information

¹ To whom correspondence should be addressed.

on the location of coke deposits arises from adsorption studies of trimethylamine and ethyldiisopropylamine; the latter is restricted to adsorption by the external surface due to its size (21). At low coke levels portions of empty channel space are sealed off while further coking produces pore filling. Almost all strong acid sites on the external surface are removed by coking deposits, which themselves give rise to new weaker acid sites (21).

Coke, produced as a result of catalytic hexane cracking over zeolite ZSM-5, formed initially within the channels and finally was deposited on the external surface, while in the case of mesitylene cracking, coke formation occurred mainly near the external surface as monitored by molecular self-diffusion (22).

A previous study has demonstrated that the number of Brønsted acid sites on the internal surface versus the number on the external surface of the ZSM-5 zeolite can be deduced from measurements of total ion-exchange capacity and cationic dye (methylene blue) adsorption capacity (23). This report describes the use of this technique to gather further information on the distribution of coke deposits arising from the conversion of methanol and mesitylene over ZSM-5 zeolites of variable trivalent metal ion type and content.

EXPERIMENTAL

Descriptions of the techniques used to synthesize and characterize the zeolites samples are reported previously in studies of the three ZSM-5 isomorphs, [Al]-ZSM-5 (24), [Ga]-ZSM-5 (25), and [Fe]-ZSM-5 (26).

Each sample was identified as ZSM-5 (MFI) structured material by the peak positions and relative intensities of its X-ray powder diffraction pattern. Other amorphous or crystalline phases were not detected in these samples. The absence of impurity phases was confirmed by scanning electron microscopy. The scanning electron microscope examination of the two

aluminum-containing zeolites, designated [Al]-ZSM-5(1) and [Al]-ZSM-5(2), showed that the constituent particles were irregular polycrystalline aggregates, 0.2 to 1.3 μm in size, composed of poorly defined crystallites less than 0.05 μm in size. Similar poorly defined crystallites with few well-formed crystal faces ($\leq 0.05 \mu\text{m}$ in size) formed the polycrystalline aggregates of the [Ga]-ZSM-5 and [Fe]-ZSM-5 samples where aggregate particle sizes were 0.3 to 1.0 and 1.0 to 4.0 μm , respectively.

Following calcination (773 K, 16 h) to remove the template molecule, all samples were treated in hydrochloric acid solution (0.5 mol dm^{-3} , 16 h refluxing) to give the proton forms H-[Al]-ZSM-5, H-[Ga]-ZSM-5, and H-[Fe]-ZSM-5. The silicon-to-trivalent metal ion ratio of each sample, calculated from the bulk chemical composition, and ion-exchange capacity (IEC) of each sample, is shown in Table 1. Also shown in Table 1 in the ratio of IEC to bulk trivalent metal ion content. This ratio is a measure of the proportion of trivalent metal ions located in the framework and forming proton exchange sites. The H-[Al]-ZSM-5(1) and H-[Ga]-ZSM-5 samples show that all the trivalent metal ions present (within experimental error) are substituted into the framework. For H-[Al]-ZSM-5(2) a small portion (8%) and for H-[Fe]-ZSM-5 a larger portion (37%) of the trivalent metal ions do not form proton-exchange sites. The methylene blue monolayer capacities and external sur-

TABLE 1

Zeolite Compositions

Sample	Si/M(III) ^a	Ion-exchange capacity ^b (mmol/100 g) ^b	Ion-exchange capacity/bulk M(III) content ^c
H-[Al]-ZSM-5(1)	39	37	0.98
H-[Al]-ZSM-5(2)	27	47	0.92
H-[Fe]-ZSM-5	39	24	0.63
H-[Ga]-ZSM-5	35	42	0.99

^a Measured by bulk chemical analysis.

^b Error in IEC measurements, ± 1 mmol/100 g.

^c Error, ± 0.02 .

TABLE 2
Physical Properties of the Zeolites

Sample	Methylene blue sorption capacity (mmol/100 g)	External surface area ^a (m ² /g)	Number of exchange sites per unit area of external surface ($\times 10^{16}$ m ⁻²)
H-[Al]-ZSM-5(1)	5.14	95 \pm 10	33 \pm 3
H-[Al]-ZSM-5(2)	5.93	103 \pm 10	35 \pm 3
H-[Fe]-ZSM-5	3.12	99 \pm 10	19 \pm 2
H-[Ga]-ZSM-5	5.65	—	—

^a From Refs. (21, 24).

face areas of the samples are recorded in Table 2.

The conditions of the coking experiment involved passage of methanol at a WHSV of 1 h⁻¹ through a bed of zeolite at 643 K and removal of samples of coked zeolite at selected intervals. Before each sample was removed, the zeolite bed was flushed by a methanol-free nitrogen stream at 643 K for 10 min. As the catalyst was removed the nitrogen flow rate was altered to maintain a WHSV of 1.0 h⁻¹. Mesitylene cracking was carried out at 803 K and at a WHSV of 0.1 h⁻¹. Qualitative analysis of the reactor product stream was carried out by off-line gas chromatography (Varian 3700) with flame ionization detectors using a 4-m \times $\frac{1}{8}$ -in.-o.d. OV-101 packed column. Regeneration of coked samples was carried out by heating at 773 K in a flow of air (50 cm³/min) for 16 h without addition of an oxidation catalyst.

Samples of coked zeolite were equilibrated over saturated calcium nitrate solution for 7 days before further measurements were performed.

The coke content of each sample was determined thermogravimetrically using a Cahn microbalance. Samples (50 mg) were heated in air to 623 K to remove adsorbed air and water and then heated to 973 K to determine the coke content.

Ion-exchange capacities were measured by passing a 1.0 mol dm⁻³ CsCl solution

down a column containing the coked samples (50 mg) and titrating the filtrate with standardized 0.01 mol dm⁻³ sodium hydroxide solution (24).

Methylene blue adsorption on the external surface of the zeolite was carried out by equilibration of the coked samples (50 mg) for 24 h at room temperature (293 K) (24). The amount of dye adsorbed was determined spectrophotometrically using a Cary UV-VIS spectrometer. Three measurements of methylene blue adsorption capacity were made for each coked sample.

Weight loss, ion-exchange capacity, and methylene blue adsorption measurements were determined for uncoked samples after treatment under identical conditions at 643 K for 16 h.

Coke content, methylene blue sorption capacity, and ion-exchange capacity are all calculated on the basis of the 973 K dried catalyst. Coked and dyed samples were observed under the optical microscope (Riechert-Jung Polyvar-Met).

RESULTS

Figure 1 shows the quantity of methanol per unit mass of catalyst required for the coking of each zeolite. H-[Al]-ZSM-5(1) showed an initially constant increment of coke buildup per unit quantity of feed up to the coke level of 9 wt%. The catalyst required a proportionally greater amount of methanol to reach a coke loading of 13 wt%

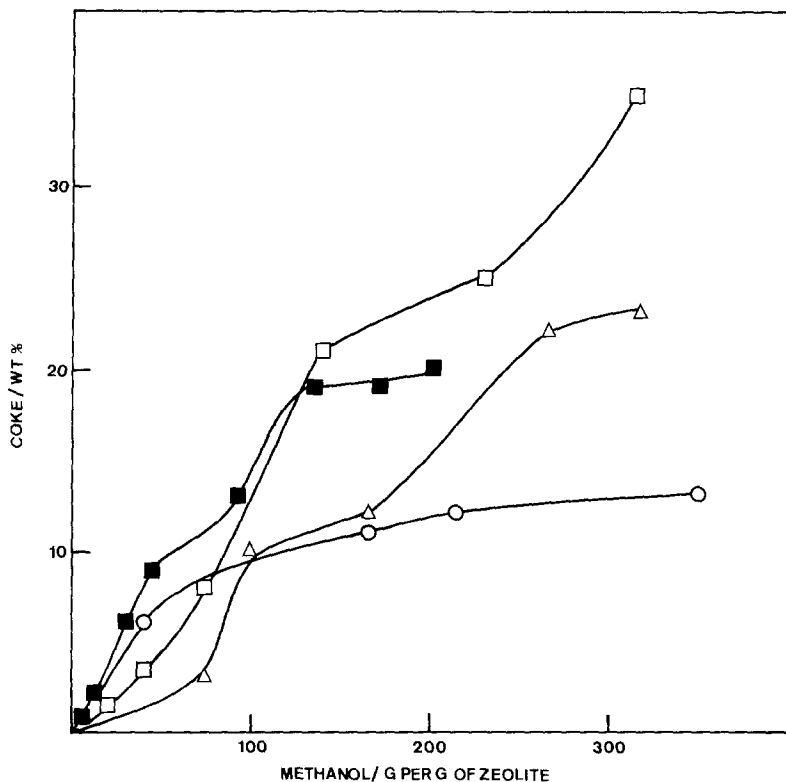


FIG. 1. Coke content of the zeolite samples H-[Al]-ZSM-5(1) (■), H-[Al]-ZSM-5(2) (□), H-[Ga]-ZSM-5 (△), and H-[Fe]-ZSM-5 (○) is plotted against quantity of methanol feed.

at which point the catalyst had ceased production of hydrocarbons (at 96 g of methanol/g of zeolite) but continued to convert methanol to dimethyl ether. Further treatment with methanol produced a final coke loading of 20 wt%. The other aluminum-containing zeolite H-[Al]-ZSM-5(2) showed a proportional increase in coke loading with the quantity of methanol feed up to the point of deactivation, 20 wt% (140 g/g). Thereafter coking increased at a greater increment per unit of feed to reach 35 wt%. By contrast, the H-[Ga]-ZSM-5 sample showed a lower increment of coke formation per unit of feed reaching the point of catalyst deactivation at 20 wt% (260 g/g). Initially, the H-[Fe]-ZSM-5 zeolite was characterized by an increment in coke formation per unit quantity of feed similar to that observed for H-[Al]-ZSM-5 zeolites. Beyond 6 wt% coke loading, the amount of

methanol required to achieve a coke level of 10 wt% was approximately the same as that required for the H-[Ga]-ZSM-5 to reach a similar level. Complete deactivation at a 13 wt% loading required the largest exposure to methanol of the four zeolites (350 g/g).

The IEC of H-[Al]-ZSM-5(1) declined proportionally with increasing coke content (up to 3 wt%) as shown by Fig. 2. Between 3 and 7 wt% loading a change in coking behavior occurred resulting in a more moderate decline in IEC. Increases in coke loading above 7 wt% caused a proportional decline in IEC up to the point of deactivation (13 wt%). Further coking, up to 20 wt%, produced a relatively small reduction of IEC (1.0 mmol/100 g), leaving a residual capacity of approximately 6.0 mmol/100 g.

Coking of H-[Al]-ZSM-5(2) to a loading of 8 wt% produced a similar rapid decline in

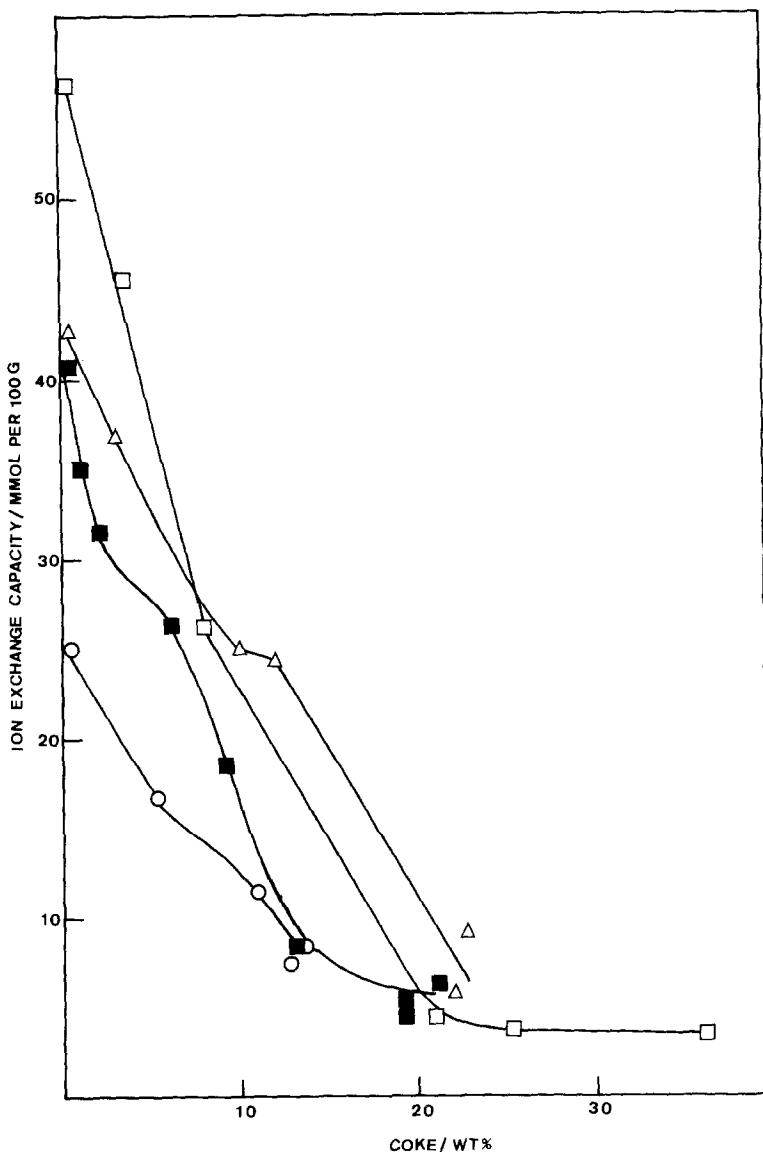


FIG. 2. Effect of coke deposition on the ion-exchange capacity for H-[Al]-ZSM-5(1) (■), H-[Al]-ZSM-5(2) (□), H-[Ga]-ZSM-5 (△), and H-[Fe]-ZSM-5 (○).

IEC to that observed in the initial stages of H-[Al]-ZSM-5(1) coke deposition. A smaller decline in the IEC resulted as the coke loading increased to 21 wt%. Beyond 20 wt% coke loading, where the IEC was 4.0 mmol/100 g, only a small change to a value of 3.5 mmol/100 g occurred as the coke content reached 35 wt%.

In a fashion somewhat similar to that ob-

served for H-[Al]-ZSM-5(1), the IEC for H-[Ga]-ZSM-5 initially declined proportionally up to a loading of approximately 9 wt%, suffered a small change as coking increased to 13 wt%, and finally steadily declined in the way initially observed. A residual IEC of approximately 8.0 mmol/100 g remained at a maximum coke loading of 22 wt%. Three stages were also observed in

the IEC behavior of H-[Fe]-ZSM-5, namely, an initial moderate decline up to a coking level of approximately 7 wt%, a small change between 7 and 10 wt%, and a resumption of the initial moderate decline to reach a residual capacity of approximately 8.0 mmol/100 g at maximum coke loading (13 wt%).

To evaluate the reproducibility of the ion-exchange capacities of the coked samples, each IEC measurement was repeated. The ion-exchange capacities determined on the second occasion were within 2% of the original values for samples with ion-exchange capacities greater than 10 mmol/100 g and within 6% for samples with ion-exchange capacities less than 10 mmol/100 g. The marked changes of slope observed with increasing coke content are outside the limits of experimental error.

Methylene blue adsorption capacity for H-[Al]-ZSM-5(1) dropped initially from 5.5 to 5.1 mol/100 g at 1 wt% coke loading (Fig. 3). A steady increase to 5.3 mmol/100 g occurred as coking reached 9 wt% and was followed by a second larger decline to 4.7 mmol/100 g between coke loadings of 11 and 20 wt%. Very different behavior was observed for H-[Al]-ZSM-5(2), which showed a large decline from 5.6 to 0.2 mmol/100 g as the coke loading reached 21 wt%. A small increase in dye adsorption capacity from 0.3 to 0.5 mmol/100 g occurred as coking reached 35 wt%.

Methylene blue adsorption capacity for H-[Ga]-ZSM-5 initially declined from 5.9 to 5.3 mmol/100 g at 5 wt% coke level. After remaining approximately constant as coking increased to 11 wt%, a small increase in the uptake of dye to a final capacity of 5.6 mmol/100 g was observed at a coking level of 22 wt%. A decline in dye adsorption capacity from 4.1 to 3.2 mmol/100 g was observed as the coke loading on H-[Fe]-ZSM-5 reached 11 wt%. At the maximum coke loading, the dye adsorption capacity had increased relatively sharply to 3.6 mmol/100 g.

The points in Fig. 3 are the averages of

the three methylene blue adsorption capacity values determined for each sample. The experimental values of any particular sample were within 2% of the calculated average for that sample. The small changes in methylene blue adsorption capacity, particularly for the H-[Ga]-ZSM-5, H-[Al]-ZSM-5(1), and H-[Fe]-ZSM-5 samples, are beyond this limit in experimental error.

Optical microscope observation of the heterogeneity or otherwise of the dyeing of the coked samples was hampered by the brown opaque coloration of the coked particles, which obscured the blue color of the dye.

Regeneration of a heavily coked sample [H-[Al]-ZSM-5(2), 35 wt% coke] gave rise to partial restoration of the ion-exchange capacity (86%) and the complete recovery of the methylene blue adsorption capacity (100%).

The relatively small quantity of coke (3 wt%) deposited during the cracking reaction of mesitylene over H-[Al]-ZSM-5(1) produced no change in either the ion-exchange capacity or the methylene blue adsorption capacity.

DISCUSSION

The measurement of ion-exchange capacity during coke formation on ZSM-5 zeolites monitors the loss of accessible ion-exchange sites, reflecting the decline in the Brønsted acidity of the samples. However, IEC measurements do not differentiate between exchange sites on the external surface and those within the channels. Given that the majority [between 75 and 85% (23)] of the ion-exchange sites are located within the channel structure, changes in IEC would arise predominantly from the effects of coke formation at these sites, with a smaller effect coming from external acid sites. More detailed information on the effects that coking has on the external acid sites is gained from changes in the methylene blue adsorption capacity (see later discussion).

By use of the data displayed in Fig. 2, the

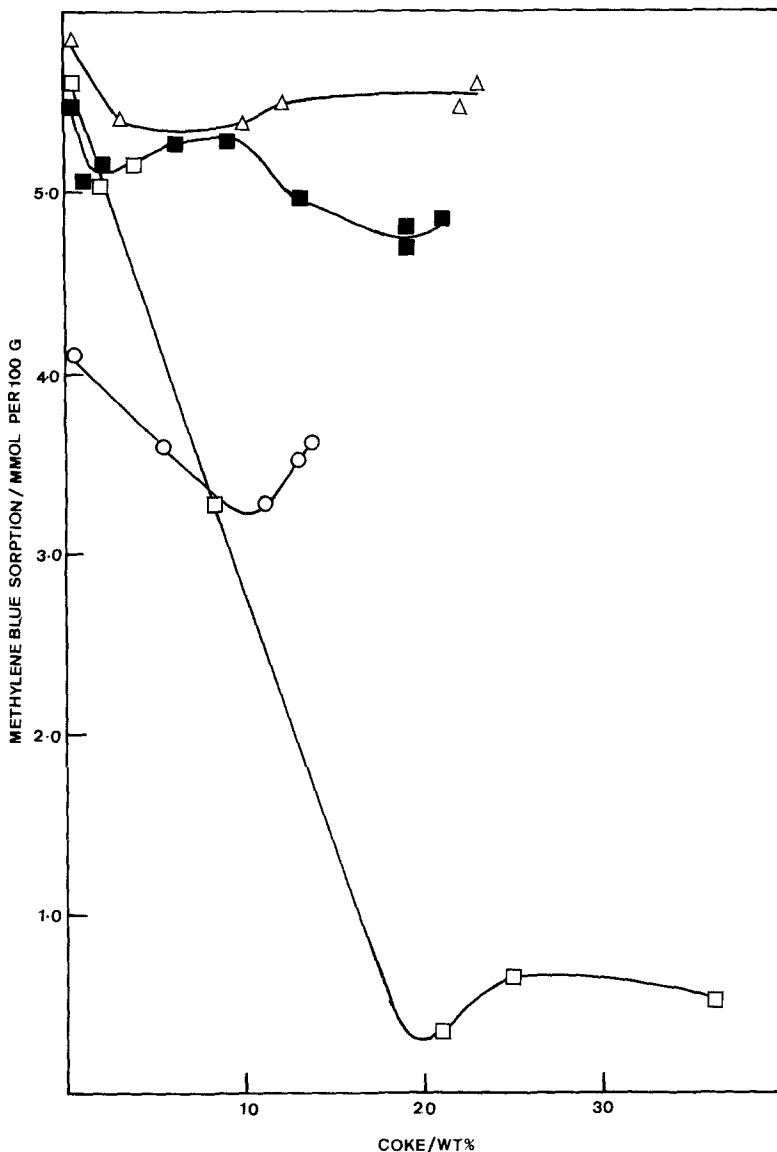


FIG. 3. Effect of coke deposition on the methylene blue adsorption capacity for H-[Al]-ZSM-5(1) (■), H-[Al]-ZSM-5(2) (□), H-[Ga]-ZSM-5 (△), and H-[Fe]-ZSM-5 (○).

number of acid sites covered per 100 carbon atoms can be approximated using $[\text{IEC} (\text{mmol}/100 \text{ g}) \times M_{\text{wc}}]/[\text{coke content} (\text{wt}\%) \times 10]$, where M_{wc} is the molecular weight of carbon. It is assumed that the coke contains only carbon atoms; the presence of a small quantity of hydrogen would not alter the result significantly.

By use of these calculations, compari-

sons can be made between the initial and final stages of acid site blocking. In the first stage of coking, the two aluminum-containing zeolites and the gallium-containing zeolite show greater acid site coverage per 100 carbon atoms [H-[Al]-ZSM-5(1), 4.4; H-[Al]-ZSM-5(2), 4.6 and H-[Ga]-ZSM-5, 2.1] compared to the final stage [H-[Al]-ZSM-5(1), 3.7; H-[Al]-ZSM-5(2) 2.0 and H-[Ga]-

ZSM-5, 1.8]. For the H-[Fe]-ZSM-5 sample, both stages of coking were characterized by the same acid site coverage (2.0 acid sites per 100 carbon atoms). Observations of similar loss of acidity at low coke content for H-[Al]-ZSM-5 zeolites have been made previously (21). Comparing the two aluminum samples, the higher the bulk aluminum content the greater the difference between the initial and final stages of acid site coverage.

The severity of decline of the first part of the curves representing the loss of acid sites as a function of coke content (Fig. 2) increases in the order H-[Fe]-ZSM-5 < H-[Ga]-ZSM-5 < H-[Al]-ZSM-5. Placed on a more quantitative basis, H-[Fe]-ZSM-5 shows the lowest coverage of acid sites per 100 carbon atoms, 2.0, followed in order of increasing coverage by H-[Ga]-ZSM-5 (2.1) and H-[Al]-ZSM-5 zeolites [sample 5 (1) 4.4 and (2) 4.6]. The relative Brønsted acid strength of the three isomorphs follows the same order, as indicated by bridging hydroxyl stretching frequencies, ammonia desorption peak maxima temperatures (27, 28), and methylene blue adsorption equilibrium constants (26). The stronger acid sites are more sensitive to poisoning by coke deposits and hence are the first to lose activity. In the final stages of coking the relatively weak sites remaining on the zeolite were less susceptible to coking, showing approximately the same lower increments of coverage (1.8–2.0 acid sites per 100 carbon atoms). The exception was H-[Al]-ZSM-5(1), where acid site coverage continued in a similar fashion (3.7 acid sites per 100 carbon atoms), pointing to acid sites of predominantly greater strength.

Apart from areas of coke-free external surface, the residual IEC remaining after the catalyst is deactivated may also arise from the presence of portions of coke-free channel structure still accessible to water molecules which facilitate ion exchange.

The dye molecule methylene blue is restricted by its size [$3.25 \times 7.6 \times 17 \text{ \AA}$ (29)] from entering the channels [5.4×5.6 and

$5.1 \times 5.4 \text{ \AA}$ (30)] of the ZSM-5 zeolite. The adsorption of this molecule by an ion-exchange mechanism (each cationic dye molecule displaces one proton) monitors the number of active Brønsted acid sites on the external surface (23). H-[Fe]-ZSM-5, H-[Ga]-ZSM-5, and H-[Al]-ZSM-5(1) all show a characteristic fall followed by a small rise in dye adsorption capacity. This relatively small effect may be accounted for by initial coke precursors blocking some external acid sites, followed by an increase in acidity as aggregation of the coke species occurs leading to the uncovering of some acid sites. Aggregation phenomena will also occur inside the pore structure; however, on the unrestricted external surface large coke precursors will migrate unhindered by the confining surfaces of the channels.

The second fall observed in the dye adsorption capacity of the H-[Al]-ZSM-5(1) sample arises from further coking of the external surface just before and following deactivation of the catalyst. Similar behavior for the H-[Ga]-ZSM-5 and H-[Fe]-ZSM-5 samples was not observed as the maximum coke loading was reached at the point of catalyst deactivation.

The uniform decline in methylene blue adsorption capacity exhibited by H-[Al]-ZSM-5(2), which contained 3.34 Al per unit cell, is evidence for the blocking by coke deposits of acid sites, preventing ion exchange from occurring at sites on the external surface. The small rise in dye adsorption after the deactivation of H-[Al]-ZSM-5(2) probably arises from the uncovering of some acid sites as aggregation occurs during further coke buildup. It has been suggested that the coke deposited once the zeolite was deactivated arises from the thermal cracking of the methanol feed (16).

Variation in the external acid site density may explain the large differences in external coke level observed for the two aluminum-containing zeolites. The number of ion-exchange sites per unit of external surface area for each H-[Al]-ZSM-5 zeolite

was calculated using the following expression $(X_m \times N_A)/(S_e \times 10^5)$, where X_m is the methylene blue monolayer capacity of each sample (mmol/100 g, Table 2), N_A is Avogadro's constant (mol^{-1}), and S_e is the external surface area (m^2/g , Table 2). The H-[Al]-ZSM-5(1) and H-[Al]-ZSM-5(2) samples have approximately the same number of exchange sites per unit area of external surface ($33 \pm 3 \times 10^{-16}$ and $35 \pm 3 \times 10^{-16} \text{ m}^{-2}$, respectively, Table 2). The degree to which coke formation occurs on the external surface must be determined by the heterogeneity of acid site distribution, which in turn is dependent on the overall aluminum content of the zeolite. The small portion of extra-framework aluminum(III) ions (8%) in H-[Al]-ZSM-5(2) may also play a role in the formation of coke on the external surface.

Previous work using ethyldiisopropylamine as a monitor for the external surface acidity of a H-[Al]-ZSM-5 zeolite sample with 2.53 aluminum ions per unit cell (Si/Al ratio of 37) (21) showed the almost total loss of strong external surface acidity at a coke loading of 23 wt%. This result is contrary to the retention of 87% of the external surface acidity observed for H-[Al]-ZSM-5(1), a sample which contained approximately the same quantity of aluminum ions per unit cell, i.e., 2.41. The variations in coking characteristics of the external surface of H-[Al]-ZSM-5 zeolite samples, due largely to the degree of heterogeneity of aluminum distribution, must arise from subtle differences in the preparation of each zeolite sample.

The removal of coke from the internal surface by heat treatment in an air stream was only partially successful as indicated by the 86% restoration of IEC. The complete restoration of methylene blue adsorption after catalyst reactivation points to the total removal of coke material from the external surface of the zeolite. These results supported previous work showing partial reactivation after treatment in oxygen or ozone (9, 10).

A marked difference exists between the effect on the H-[Al]-ZSM-5(1) sample of coke produced from mesitylene cracking and that from the methanol conversion. No change in IEC and methylene blue adsorption was observed after mesitylene cracking, while coking to a similar level (3 wt%) by methanol produced marked changes in IEC (42 to 31 mmol/100 g) and methylene blue adsorption capacity (5.5 to 5.1 mmol/100 g). This evidence suggests that coke deposits produced by mesitylene cracking differ in location and/or nature compared to coke originating from the methanol conversion. ^1H NMR diffusion measurements suggest that the coke formed on the ZSM-5 zeolites by the mesitylene cracking reaction was situated near the external surface (22). Evidence presented in this study shows that exchange sites at this location were not physically blocked by the coke or the chemical nature of the coke allows that alkali ion and dye cation exchange to occur unhindered.

REFERENCES

1. Cormerais, F. X., Perot, G., and Guisnet, M., *Zeolites* **1**, 141 (1981).
2. Guisnet, M., Magnoux, P., and Canaff, C., *Stud. Surf. Sci. Catal.* **28**, 701 (1986).
3. Eisenbach, D., and Gallei, E., *J. Catal.* **56**, 377 (1979).
4. Dejaifve, P., Auroux, A., Gravelle, P. C., Védrine, J. C., Gabelica, Z., and Derouane, E. G., *J. Catal.* **70**, 123 (1981).
5. Walsh, D. E., and Rollman, L. D., *J. Catal.* **56**, 195 (1979).
6. Marquart, R., and Fetting, F., *Chem. Ing. Technol.* **57**, 982 (1985).
7. Yurchak, S., Voltz, S. E., and Warner, J. P., *Ind. Eng. Chem. Process Des. Dev.* **18**, 527 (1979).
8. Magnoux, P., and Guisnet, M., *Appl. Catal.* **38**, 341 (1988).
9. Copperthwaite, R. G., Hutchings, G. J., Johnston, P., and Orchard, S. W., *J. Chem. Soc. Chem. Commun.*, 664 (1985).
10. Copperthwaite, R. G., Hutchings, G. J., Johnston, P., and Orchard, S. W., *J. Chem. Soc. Faraday Trans. 1* **82**, 1007 (1986).
11. Copperthwaite, R. G., Foulds, G., Themistocleous, T., and Hutchings, G. J., *J. Chem. Soc. Chem. Commun.*, 748 (1987).
12. Hutchings, G. J., Comminos, H., Copperthwaite,

- R. G. Rensburg, L. J., Hunter, R., and Themistocleous, T., *J. Chem. Soc. Faraday Trans. 1* **85**, 633 (1989).
13. Derouane, E. G., Gilson, J-P., and Nagy, J. B., *Zeolites* **2**, 42 (1982).
 14. Schulz, H., Siwei, Z., and Baumgartner, W., *Stud. Surf. Sci. Catal.* **34**, 479 (1987).
 15. Magnoux, P., Roger, P., Canaff, C., Fouche, V., Gnep, N. S., and Guisnet, M., *Stud. Surf. Sci. Catal.* **34**, 317 (1987).
 16. Bibby, D. M., Milestone, N. B., Patterson, J. E., and Aldridge, L. P., *J. Catal.* **97**, 493 (1986).
 17. McLellan, G. D., Howe, R. F., Parker, L. M., and Bibby, D. M., *J. Catal.* **99**, 486 (1986).
 18. Bibby, D. M., McLellan, G. D., and Howe, R. F., *Stud. Surf. Sci. Catal.* **34**, 651 (1987).
 19. Sexton, B. A., Hughes, A. E., and Bibby, D. M., *J. Catal.* **109**, 126 (1988).
 20. Behrsing, T., Jaeger, H., and Sanders, J. V., *Appl. Catal.* **54**, 289 (1989).
 21. Bibby, D. M., and Pope, C. G., *J. Catal.* **116**, 407 (1989).
 22. Bülow, M., Caro, J., Völter, J., and Kärger, J., *Stud. Surf. Sci. Catal.* **34**, 343 (1987).
 23. Handreck, G. P., and Smith, T. D., *J. Chem. Soc. Faraday Trans. 1* **84**, 645 (1989).
 24. Handreck, G. P., and Smith, T. D., *J. Chem. Soc. Faraday Trans. 1* **84**, 4191 (1988).
 25. Handreck, G. P., and Smith, T. D., *J. Chem. Soc. Faraday Trans. 1* **85**, 3215 (1989).
 26. Handreck, G. P., and Smith, T. D., *J. Chem. Soc. Faraday Trans. 1* **85**, 3195 (1989).
 27. Chu, C. T-W., and Chang, C. D., *J. Phys. Chem.* **89**, 1569 (1985).
 28. Gricus Kofje, T. J., Gorte, R. J., and Kokotailo, G. T., *J. Catal.* **166**, 252 (1989).
 29. Hang, P. T., and Brindley, G. W., *Clays Clay Miner.* **18**, 203 (1970).
 30. Olson, D. H., Kokotailo, G. T., Lawton, S. L., and Meier, W. M., *J. Phys. Chem.* **85**, 2238 (1981).